Supplementary Information

for

Highly efficient ethanol vapour detection using g-C_3N_4/ZnO micro flower-like heterostructural composites

Xianfeng Zhang, Wenjie Du, Qian Li, Changpeng Lv*

Anhui Provincial Engineering Laboratory of Silicon-based Materials and School of Material and Chemical Engineering, Bengbu University, Bengbu 233030, People's Republic of China

Corresponding author. Tel: +86 552 3179368

E-mail address: lvcp1213@gmail.com

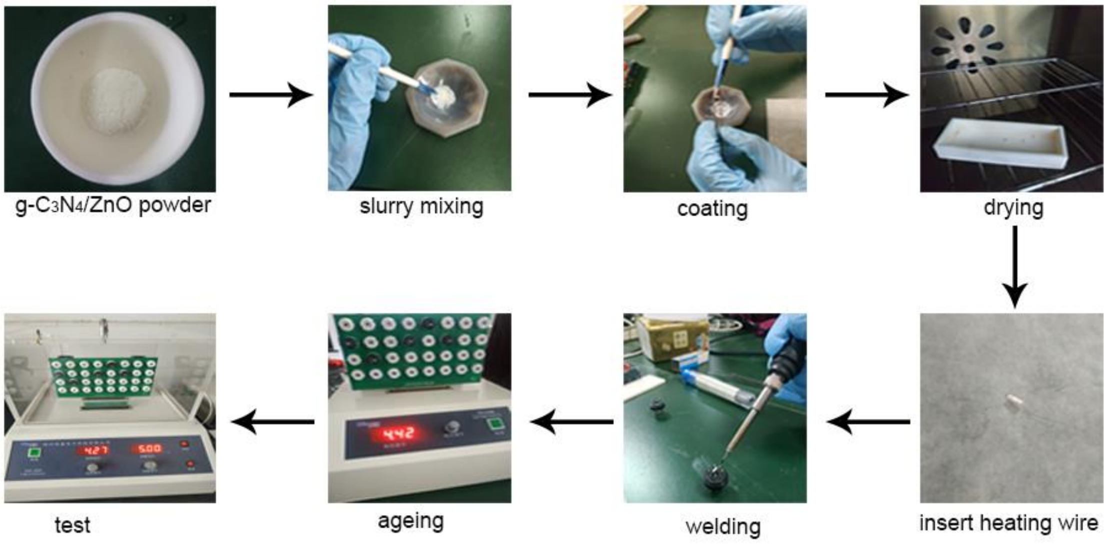

Figure S1. Schematic diagram of ethanol vapor sensor fabrication process.

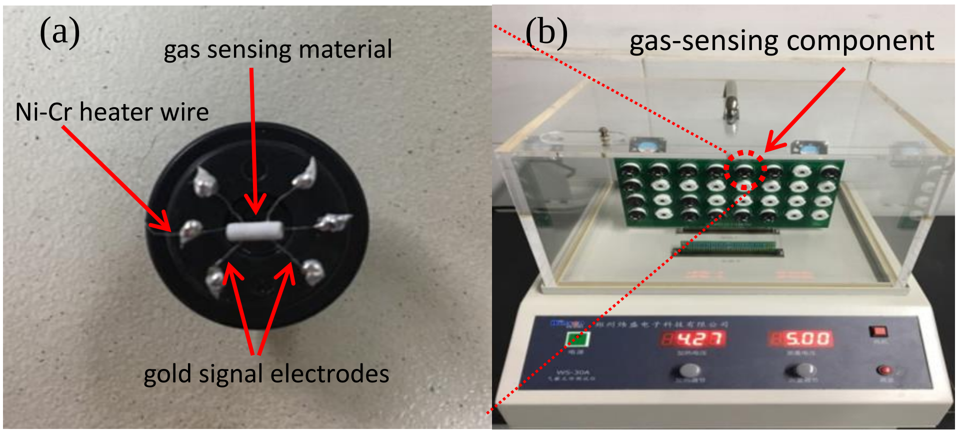

Figure S2. (a) The prepared g-C_3N_4/ZnO gas sensor component. (b) The gas-sensing component test system for examing gas-sensing properties of the synthesized materials.

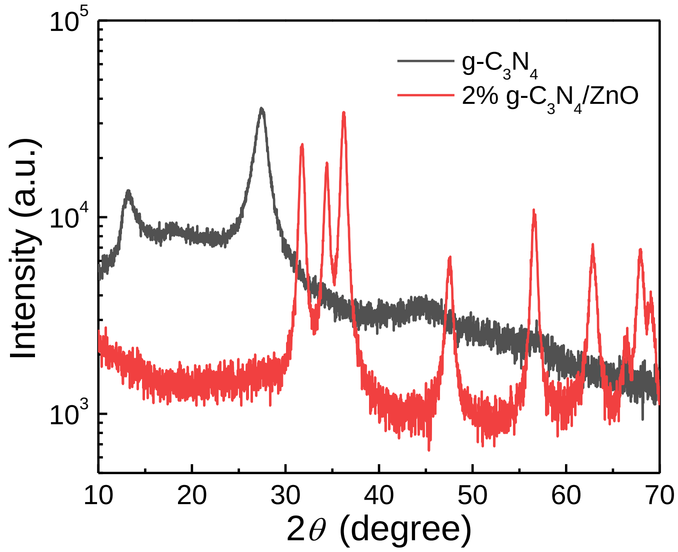

Figure S3. XRD patterns of the g-C_3N_4 and 2%g-C_3N_4/ZnO composite in logarithmic scale.

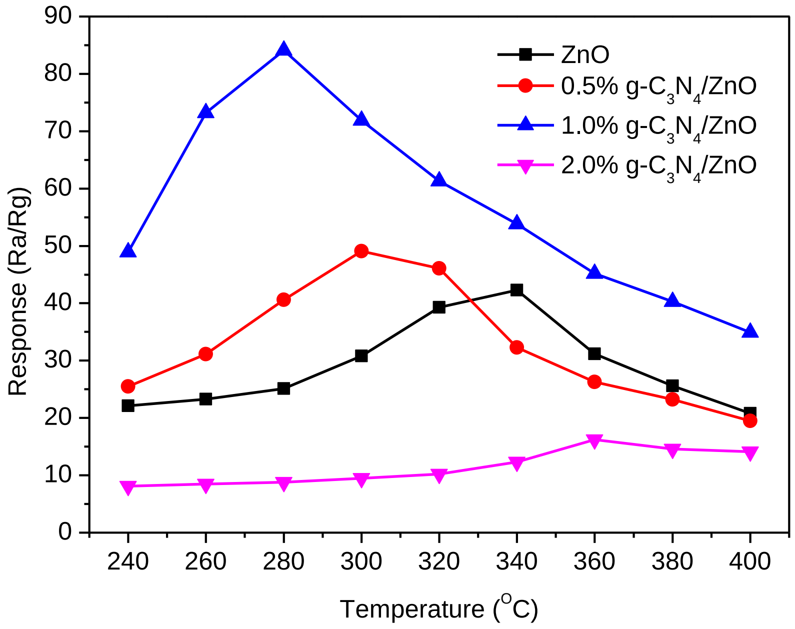

Figure S4. Response of ZnO and C_3N_4/ZnO composite gas sensors to 100 ppm ethanol vapour at different working temperatures.

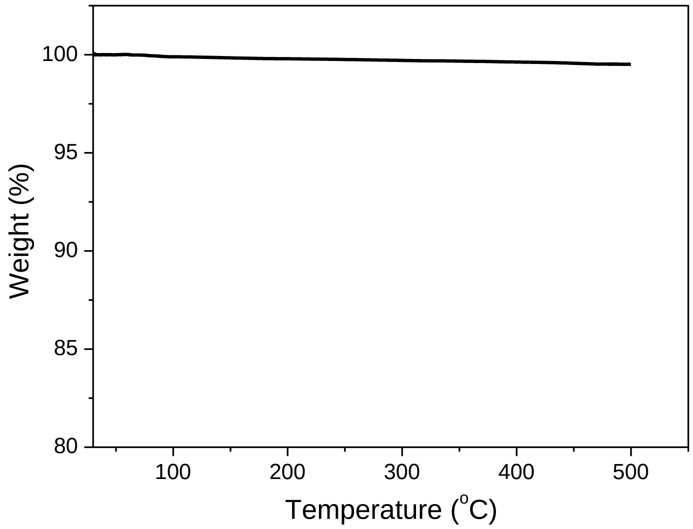

Figure S5. TGA curves of 1%g-C_3N_4/ZnO composite.

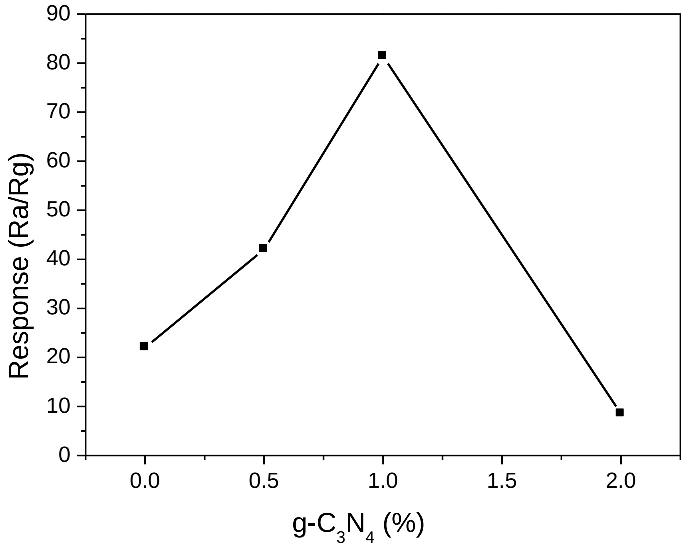

Figure S6. Response value relationship of g-C_3N_4/ZnO gas sensor with different g-C_3N_4 doping content to 100 ppm ethanol.

Table S1. The Ra values of ZnO and g-C_3N_4/ZnO composites at different operating temperatures.

Working temperatures (°C)	Ra values of ZnO (KΩ)	Ra values of 1%g-C_3N_4/ZnO composites (KΩ)
240	41332.09	572256.71
260	32718.03	363443.70
280	28211.37	131746.58
300	24329.13	58058.68
340	21242.80	29589.12
380	13925.73	10776.73
400	11847.18	8552.31

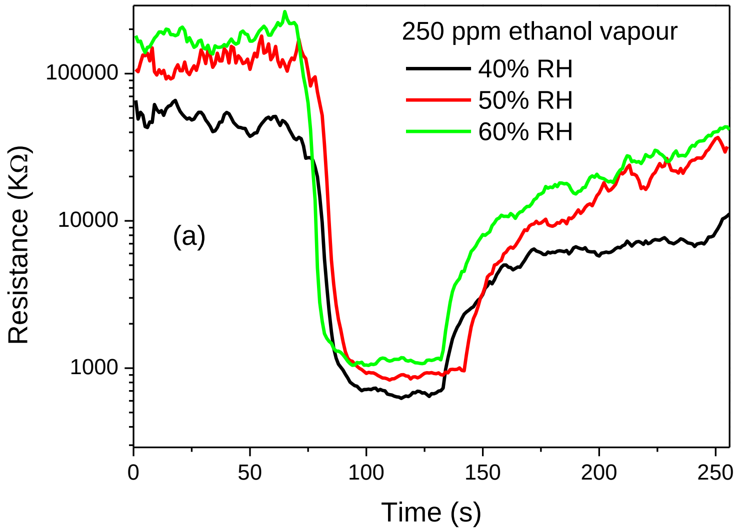

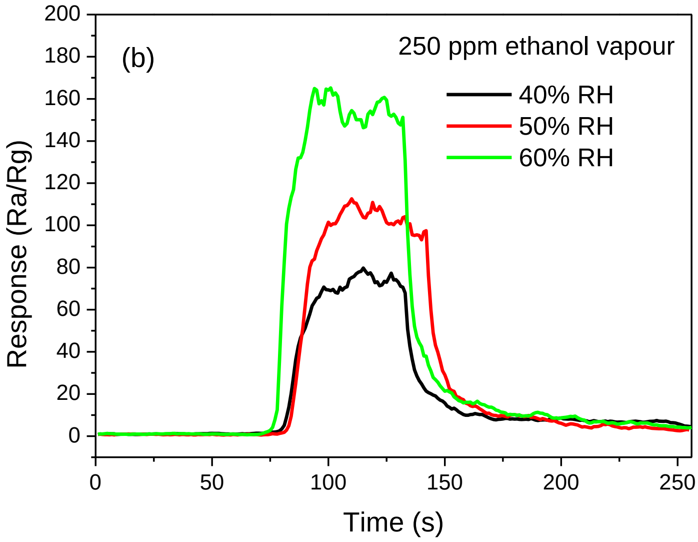

Figure S7. (a) The dynamic resistance curve of the 1% g-C_3N_4/ZnO composite to 250 ppm ethanol vapour at optimal working temperature at various relative humidities. (b) Dynamic response at various humidity levels.

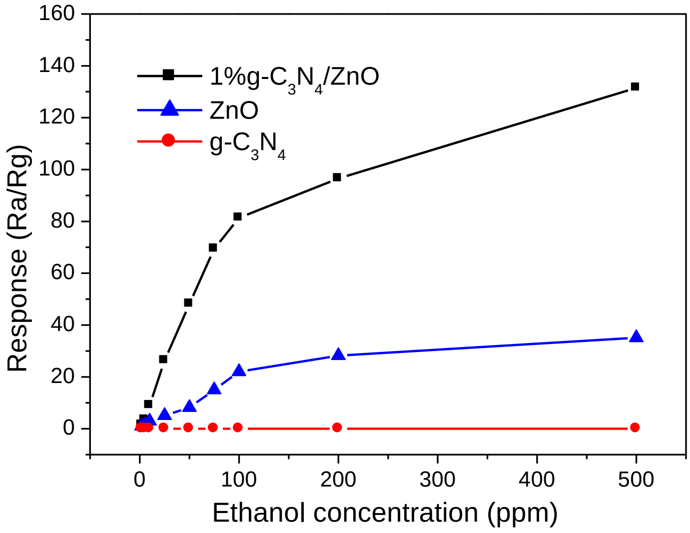

Figure S8. Response of the 1% g-C_3N_4/ZnO, ZnO, and g-C_3N_4 gas sensors to different concentrations of ethanol vapour.

Table S2. The Ra (or Rg) values of 1%g-C_3N_4/ZnO composites and corresponding response value to different ethanol vapour concentrations.

Concentrations of ethanol vapour (ppm)	Ra (or Rg) values of g-C_3N_4/ZnO composites (KΩ)	Response (Ra/Rg)
0	133786.96	1
2	88571.26	1.51
5	38639.36	3.46
10	14854.55	9.01
25	5076.20	26.36
50	2777.45	48.17
75	1926.81	69.43
100	1643.57	81.40
200	1385.60	96.56
500	1017.54	131.48

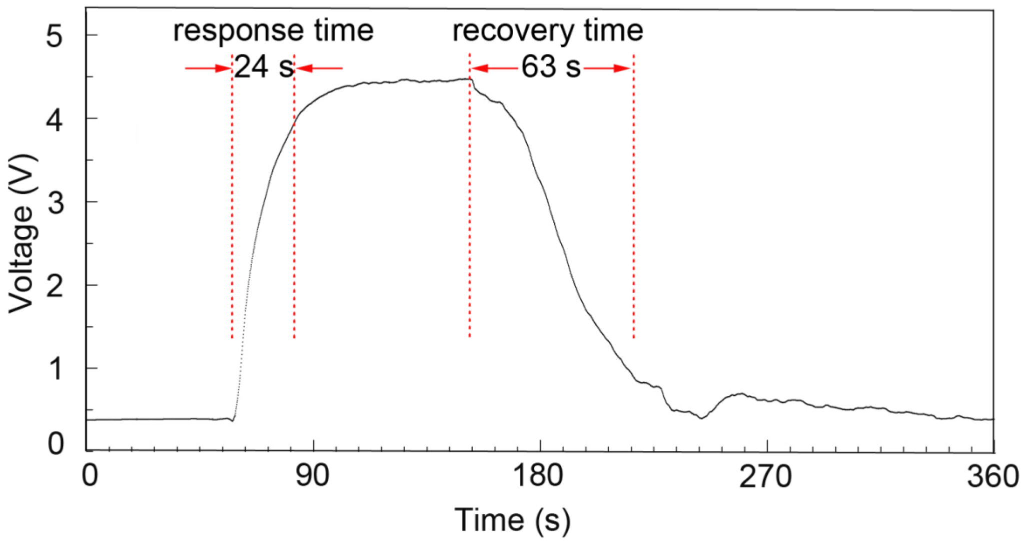

Figure S9. Response recovery curve of 1% g-C_3N_4/ZnO gas sensor to 100 ppm ethanol vapour.

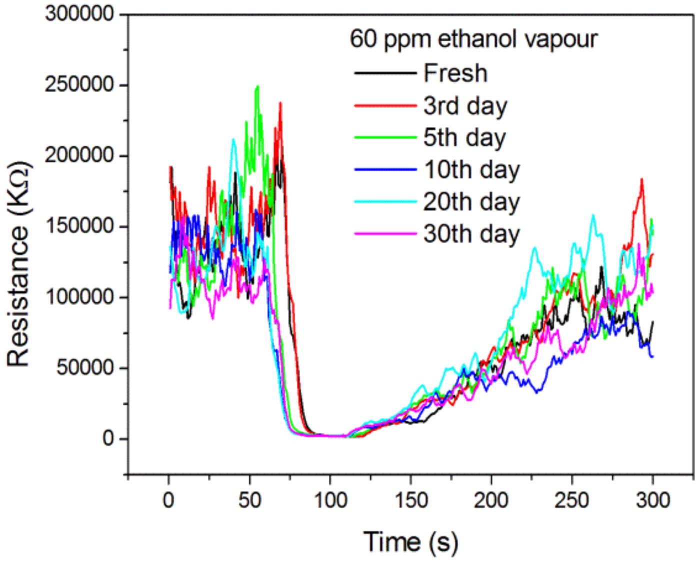

Figure S10. The dynamic resistance curves of the fresh sensor and the sensor stored for different time.

Table S3. The Ra values, Rg values and Response value of the fresh sensor and the sensor stored for different time.

Storage time (day)	Ra values of $g\text{-}C_3N_4/ZnO$ composites (KΩ)	Rg values of $g\text{-}C_3N_4/ZnO$ composites (KΩ)	Response value (S=Ra/Rg)
fresh	140525.70	2658.95	52.85
3rd	138528.53	2655.32	52.17
5th	136853.08	2655.23	51.54
10th	135601.89	2733.58	49.60
20th	133662.10	2769.60	48.26
30th	114604.20	2504.10	45.76

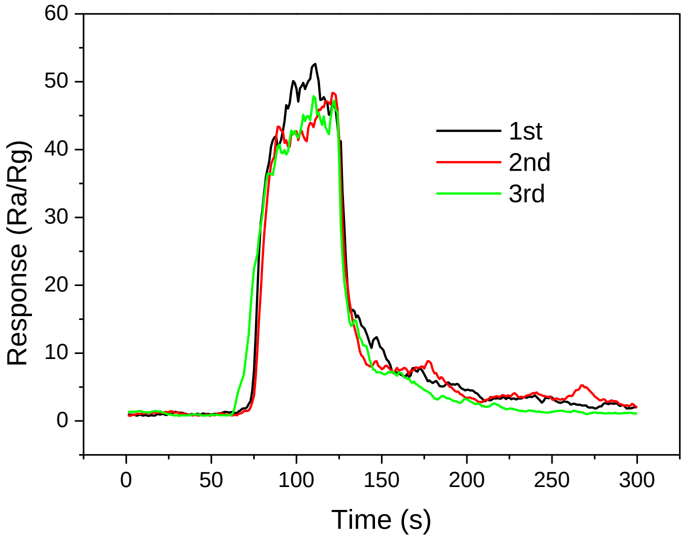

Figure S11. The repeatability of the 1% g-C_3N_4/ZnO composite based sensor to 50 ppm ethanol vapour.

Table S4. The comparative analysis of the sensing performances between this work and the previously reported results.

Sensing materials	Ethanol concentration (ppm)	Temperature (℃)	Response (Ra/Rg)	Ref.
3D SnO_2 nanoflower	100	240	7	[S1]
Au/3D SnO_2 microstructure	150	340	30	[S2]
RGO/hollow SnO_2	100	300	70.4	[S3]
Pt/3D SnO_2 nanoflower	100	320	8	[S4]
SnO_2/g-C_3N_4	100	300	105	[S5]
Cocoon-like ZnO/ g-C_3N_4	100	350	15.8	[S6]
g-C_3N_4/ZnO micro flower	100	280	81.4	This work

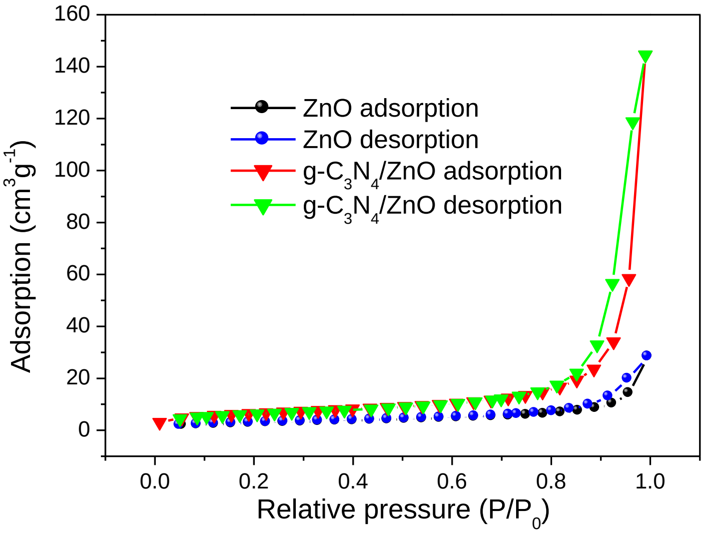

Figure S12. N_2 adsorption-desorption isotherms for the ZnO and 1%g-C_3N_4/ZnO composite.

References:

S1. L. Wang, S. Wang, Y. Wang, H. Zhang, Y. Kang, W. Huang, Synthesis of hierarchical SnO_2 nanostructures assembled with nanosheets and their improved gas sensing properties, *Sens. Actuators B*, 2013, **188**, 85–93.

S2. J. Guo, J. Zhang, H. B. Gong, D. X. Ju, B. Q. Cao, Au nanoparticle-functionalized 3D SnO_2 microstructures for high performance gas sensor, *Sens. Actuators B*, 2016, **226**, 266–272.

S3. C. A. Zito, T. M. Perfecto, D. P. Volanti, Impact of reduced graphene oxide on the ethanol sensing performance of hollow SnO_2 nanoparticles under humid atmosphere, *Sens. Actuators B*, 2017, **244**, 466–474.

S4. Y. Liu, J. Huang, J. Yang, S. Wang, Pt nanoparticles functionalized 3D SnO_2 nanoflowers for gas sensor application, *Solid State Electron.*, 2017, **130**, 20–27.

S5. J. L. Cao, C. Qin, Y. Wang. Synthesis of g-C_3N_4 nanosheets decorated flower-like tin oxide composites and their improved ethanol gas sensing properties. *J. Alloy. Compd.*, 2017, **728**, 1101–1109.

S6. J. Cao, Y. Gong, Y. Wang, B. Zhang, H. Zhang, G. Sun, H. Bala, Z. Zhang, Cocoon-like ZnO decorated graphitic carbon nitride nanocomposite: Hydrothermal synthesis and ethanol gas sensing application, *Mater. Lett.*, 2017, **198**, 76–80.